Macromolecules

Open Access

This article is licensed under CC-BY 4.0

pubs.acs.org/Macromolecules

Article

Solution Behavior of Semiflexible Polyelectrolyte Carboxymethylcellulose with Anisotropic Counterions That Have Spatially Separated Charges

Can Hou, Max Hohenschutz, Takaichi Watanabe, Walter Richtering, and Carlos G. Lopez*

Cite This: *Macromolecules* 2026, 59, 12025−12034

Read Online

ACCESS | Metrics & More | Article Recommendations | Supporting Information

ABSTRACT: The properties of polyelectrolytes depend on the counterions that neutralize their backbone. Although the effects of counterion valence and size have been studied, the influence of charge topology, i.e., the spatial distribution of charge within a multivalent counterion, has not been investigated experimentally. We address this question by comparing aqueous solutions of carboxymethyl cellulose (CMC) containing conventional divalent metal ions with solutions containing the organic ditopic counterions hexamethonium and suxamethonium. Conductivity measurements indicate comparable counterion dissociation at low polymer concentrations but substantially greater dissociation of the ditopic ions at higher concentrations. SAXS measurements reveal corresponding structural differences: CMC with ditopic counterions exhibits correlation peaks and smaller stretching parameters, consistent with a larger effective polymer charge and reduced local chain folding, whereas CMC with monotopic divalent metal counterions displays broad correlation shoulders, consistent with weaker electrostatic correlations. Partially "dangling" condensed ditopic ions provide a possible explanation for the observation that the monotopic and ditopic counterions show similar fractions of free counterions from conductivity at low concentrations, while the SAXS profiles indicate a higher effective charge for the ditopic salts. However, this mechanism cannot be established unambiguously from the present conductivity and scattering measurements. Overall, the results demonstrate that counterion charge topology provides a tuneable parameter for controlling polyelectrolyte conformation and charge transport.

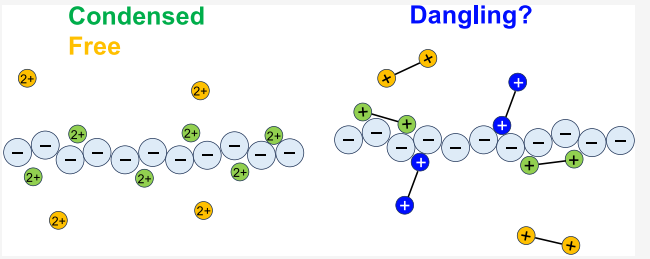

■ INTRODUCTION

The properties of polyelectrolyte solutions depend on the nature of the counterions neutralising the polymer backbone.[1] Counterion valence provides the most obvious example. Divalent counterions condense onto the backbone to approximately twice the extent of monovalent ones,[2−4] leading to lower effective backbone charges. This results in lower osmotic pressures and reduced chain dimensions.[5−9] Beyond valence, counterion-solvent interactions can also be used to tune the phase behaviour,[1,10,11] charge transport[12,13] and interfacial[14] properties of polyelectrolyte solutions and gels. Understanding which counterion properties govern these effects is therefore essential for designing charged polymers with targeted properties.

For counterions of the same valence, differences in behaviour may arise from their size and solvation. The finite size of ions sets a minimum distance of closest approach, which influences the spatial distribution of counterions around the polymer backbone. Based on this, Oosawa[15] predicted that larger counterions exhibit a higher degree of dissociation than smaller ones. In aqueous solution, however, the effective size and interaction of an ion with the backbone are also affected by its hydration shell.[16−25] Hydration influences ion pairing and has been proposed to contribute to properties such as ion selectivity in polyelectrolyte solutions and gels.[26,27]

Despite the differences in ion size and solvation, experiments show that the degree of counterion dissociation is often remarkably insensitive to the identity of monovalent counterions. The various alkali metals and ammonium ions, for example, have substantial differences in solvation shell structure,[29] yet their salts of anionic polyelectrolytes exhibit only small differences in the fraction of dissociated counterions. Figure 1 illustrates this for polystyrene sulfonate (PSS), showing the electrical conductivity of various PSS salts as a function of concentration, together with the fraction of monomers with a free counterion inferred from the conductivity data from Szymczak et al.[12] The differences among the monovalent salts are at most approximately 10%.

Received: July 9, 2026
Revised: August 23, 2026
Accepted: September 9, 2026
Published: October 23, 2026

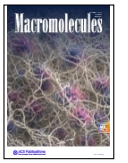

ACS Publications

© 2026 The Author(s). Published by American Chemical Society

https://doi.org/10.1021/acs.macromol.6c01930
Macromolecules 2026, 59, 12025−12034

Downloaded from pubs.acs.org/mamobx/article-pdf/59/21/12025/6970982/ma-2026-01930q.pdf by OKAYAMA UNIV user on 27 November 2026

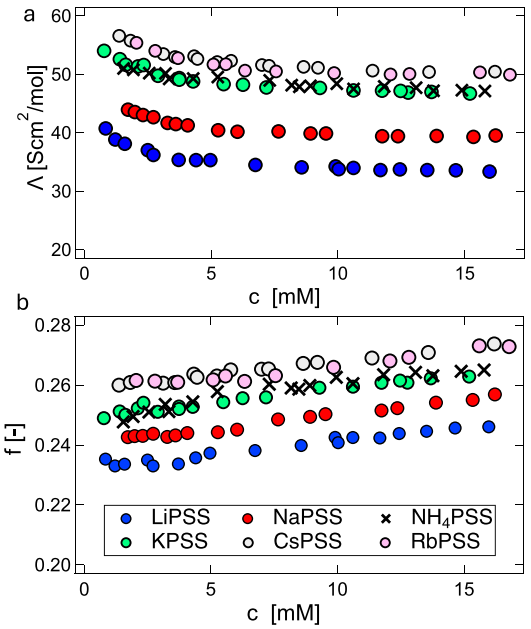

Figure 1. (a) Equivalent conductivity of PSS solutions, data from ref 12. (b) Fraction of monomers with a free counterion calculated with the model of Colby et al.[28] using ξ [Å] = 33 $c^{-1/2}$ for all salts, where c is in units of moles of repeating units per dm^3.

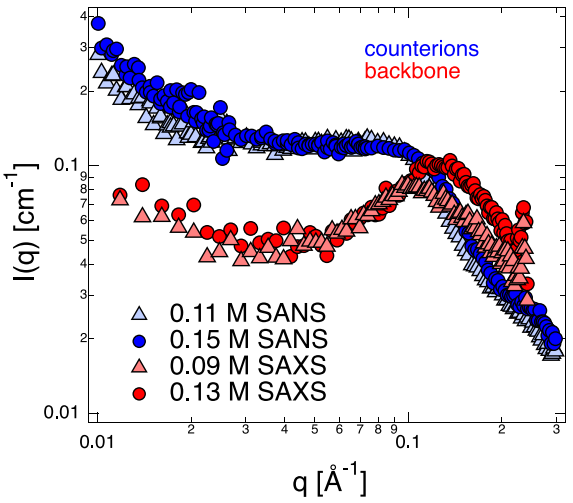

Figure 2. SANS and SAXS intensities of tetrabutylammonium carboxymethylcellulose (TBACMC) solutions in deionised (DI) water or D_2O without added salt. In SANS, the scattering signal is dominated by the contribution from the counterions and in SAXS from the polymer backbone. SANS data are in absolute units of cm^{-1} and SAXS data are in arbitrary units shifted to match the SANS data for clarity. The counterions appear to be less strongly correlated, and therefore more delocalised, than the polymer chains. Data from ref. 37.

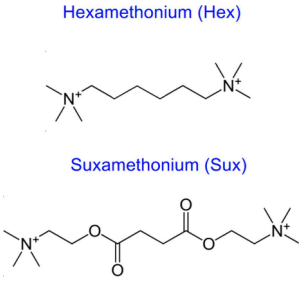

Figure 3. Structure of the two ditopic counterions used in this study: hexamethonium (Hex) and suxamethonium (Sux).

Our recent studies of the semiflexible polyelectrolyte carboxymethyl cellulose (CMC) show a similar distinction between the number of free counterions and their spatial organisation. Counterion-solvent affinity can have pronounced effects on macroscopic behaviour: large, hydrophobic counterions promote solubility in non-aqueous media,[11] whereas the viscosity, scattering, and thermodynamic properties of different monovalent salts of CMC in water are largely independent of ion identity.[4,30,31] A similar insensitivity to ion type has been reported for alkaline earth salts of CMC, where the osmotic coefficient remains approximately constant across different cations,[32,33] in line with experimental reports for other polysaccharides.[34–36] Counterion identity can nevertheless affect the spatial distribution of the free ions. At high concentrations, CMC salts with hydrophobic counterions exhibit a decoupling of polymer and counterion concentration fluctuations. An example of this behaviour is shown in Figure 2. Such behaviour is not observed for hydrophilic counterions such as alkali-metal ions.[37] Thus, counterion-solvent interactions can modify the organisation of free counterions around the polymer backbone even when the overall fraction of free counterions, as evaluated from conductivity, remains largely unchanged.[31]

These observations raise a broader question: which counterion characteristics, beyond valence and solvent affinity, can alter counterion organisation and condensation? One potentially important variable is the spatial distribution of charge within a multivalent counterion. Unlike divalent metal ions, where the charge is localized at a single center, organic anisotropic counterions can be ditopic, with two unit charges associated with spatially separated functional groups within the same molecule. Two examples of such ditopic counterions, hexamethonium and suxamethonium (also known as succinyl choline), are shown in Figure 3. While the different structure and length of the spacer between the two end groups can lead to slight differences in the local electrostatic-potential distribution between Hex and Sux, one can safely assume that the two cationic charges of the molecule will be located predominantly at the two ammonium groups at the ends.

Earlier simulation studies have investigated the effect of counterion-solvent affinity[38–40] and counterion size.[41,42] For instance, while poly(acrylic acid) (PAA) chains are always repulsive to each other, with the addition of a certain amount of calcium ions PAA-Ca^{2+}-PAA bridges can form, which is reflected in the emergence of an interaction free-energy minimum at certain interchain separation distances.[43] Moreover, the influence of counterion shape and charge distribution of multivalent counterions has been studied theoretically and by simulations for charged planar surfaces and cylindrical polyions.[44–49] Depending on the separation between charges and coupling parameter ($u = l_B/d$, where l_B is the Bjerrum length and d is the distance between charges), anisotropic counterions can generate attractive forces between planar surfaces through bridging interactions. For cylindrical polyions, Cha et al.[49] showed that idealised divalent, rod-like counterions with

https://doi.org/10.1021/acs.macromol.6c01930
Macromolecules 2026, 59, 12025−12034

Downloaded from pubs.acs.org/macromolecules/article-pdf/59/21/12025/6897082/ma-2026-01930q.pdf by OKAYAMA UNIV user on 27 November 2026

charges placed at opposite ends can interpolate between monovalent-like and divalent-like behaviour. When the distance from the polyion is smaller than the separation between the two charges, they behave effectively as two monovalent counterions, whereas at distances much larger than the separation between charges they behave as a point-like divalent ion. Although this representation neglects the detailed distribution of partial charges within real molecular ions, it provides a useful limiting description of how spatial separation of the two cationic groups can influence their interaction with a polyion.

In this study, we compare the scattering and electrical conductivity of carboxymethyl cellulose with hexamethonium and suxamethonium counterions to those of CMC with conventional monotopic counterions, including alkali and alkaline earth metal ions, where the charges are localized around a single point. Combining scattering and conductivity data allows us to estimate the fraction of free counterions as a function of concentration. The differences in scattering and conductivity are explained in terms of the fraction of free counterions, which is larger for ditopic counterions relative to monotopic ones such as Mg^{2+}. Our results show that charge topology can be used as a design variable to tune polyelectrolyte solution properties.

■ MATERIALS AND METHODS

Preparation of CMC Salts

Hexamethonium bromide ($HexBr_2$) (Sigma Aldrich) was added to approximately 0.2 M sodium carboxymethyl cellulose (NaCMC) aqueous solution, with a molar ratio of $HexBr_2$ to NaCMC monomers of more than 10:1. The NaCMC used was from the same batch used in ref 50, with the degree of substitution estimated to be 0.98 and a molar mass of 360 kg/mol, determined by static light scattering.[50] After the mixture was thoroughly dissolved and became homogeneous, it was dialysed against DI water using membranes with MWCO = 12–14 kDa obtained from SpectraPor. The de-ionised water used for the dialysis was obtained from an Astacus^2 Ultra Pure Water System (MembraPure GmbH). The filled dialysis membrane is sealed and submerged in the deionised (DI) water, with the water periodically replaced until the conductivity reaches approximately 10^{-4} S m^{-1}, which corresponds roughly to the conductivity of fresh de-ionised water. The same procedure was carried out for the ion exchange of NaCMC into divalent metal salts using calcium bromide dihydrate (Sigma Aldrich), Cobalt Nitrate (Puriss p.a. ACS Reagent, ≥99.0%, Sigma Aldrich), Manganese(II) chloride tetrahydrate (VWR, ACS Reagent), or zinc chloride (ultra dry, 99.99% metal basis) as the excess salt. Addition of a large excess of divalent metal ions led to precipitation of CMC. The entire mixture, including both precipitate and supernatant, was transferred to the dialysis bag. As the dialysis proceeds, the precipitate re-dissolves. The exception is $ZnCl_2$: addition of a large excess of zinc ions does not precipitate the polymer. As the dialysis proceeds, the polymer precipitates and then redissolves, indicating the existence of a re-entrant phase. Such behaviour has been observed for other polyelectrolytes in the presence of trivalent and tetravalent ions.[51−53] Suxamethonium dichloride of >99% purity was used for ion exchange to produce SuxCMC, and was also obtained from Sigma Aldrich. After dialysis, the polymers were freeze-dried and solutions were prepared gravimetrically. To check that the counterion exchange was complete with the above procedure, the HexCMC salt was dissolved in DI water, a 10-fold excess of $HexBr_2$ was added, followed by dialysis against DI water. The conductivity properties of the twice-exchanged and the singly exchanged HexCMC were found to be identical. The tetra-alkyl-ammonium salts of CMC used are the same polymers prepared in reference 11.

Hansen Solubility Parameter (HSP) Phase Mapping

The experimental setup for phase mapping was described in our previous work.[11] In essence, approximately 1 wt % of the polymer was placed and sealed in a 5 mL transparent glass vial with an organic solvent or solvent mixture. The mixture was left for approximately 48 h, after which the solubility status was recorded:

- Soluble: the solution is fully transparent and homogeneous with no lumps or fragments visible.
- Insoluble: the initial piece of polymer placed remains mostly intact; no changes in the colour or opacity are observed.
- Partially soluble: there is a noticeable lump in the solution, or the solution is turbid but otherwise well mixed.

All non-aqueous solvents were obtained from Sigma Aldrich. The purity of all non-aqueous solvents used is listed in Table 2 of the SI.

Synchrotron Small-Angle X-ray Scattering (SAXS)

SAXS measurements on CMC with anisotropic counterions were conducted at Beamline BL40B2 at SPring-8, Sayo, Japan. The temperature was set to 25 °C, which was maintained by a Peltier heating unit. Acquisition times were set to 1 minute. The beam energy was 12.4 keV. The sample-to-detector distance was set to 1 or 2 m. For each sample, the scattering and transmission were recorded simultaneously. The scattering intensity was radially averaged and the intensity from the capillary was then subtracted using standard reduction procedures. The SAXS data are reported in arbitrary units.

In-House Small Angle X-ray Scattering (SAXS)

SAXS measurements on CMC with symmetric metal ions were performed on a 3-pinhole S-Max3000 system with a MicroMax002+ X-ray microfocus generator from Rigaku. Samples were irradiated with Cu K_α radiation (λ = 0.154 nm). The scattered beam was recorded using a two-dimensional multi-wire detector (Gabriel design, 2D-200X with an active diameter of 200 mm) placed at a sample-to-detector distance of 2.6 m. A q-range of 0.05 to 4 nm^{-1} was covered with an off-center detection. Sealed 1.5 mm borosilicate capillaries from WJM Glas Müller GmbH served as sample containers. The magnitude of the scattering vector q was calibrated using Silver behenate. The scattered intensity was corrected for dark noise, sample transmission and capillary thickness and was brought to absolute scale using a polyethylene standard.

Small-Angle Neutron Scattering (SANS)

SANS measurements were performed on the LOQ beamline (ISIS neutron source, Didcot, UK) operating in time-of-flight mode with a white beam with a wavelength range of 2.7–10.5 Å. The sample-to-detector distance was 4 m and the beam size 8 mm. Samples were loaded into cylindrical quartz cells of 2 mm path length and the data were reduced and solvent subtracted using standard procedures.

Downloaded from pubs.acs.org/mamobx/article-pdf/59/21/12025/6970982/ma-2026-01930q.pdf by OKAYAMA UNIV user on 27 November 2026

https://doi.org/10.1021/acs.macromol.6c01930
Macromolecules 2026, 59, 12025−12034

Electrical Conductivity

A SevenMulti Dual pH/conductivity meter (Mettler Toledo) was used for the conductivity measurements. The probe used was Cond Sensor InLab 710 (Mettler Toledo). The measurements were done at 25 °C, with the temperature controlled by placing the sample container in a temperature-controlled water bath. The conductivity probe was inserted into 10 mL polypropylene vials filled with approximately 4 mL of sample solutions, with the temperature sensor fully submerged. Readings were taken when the apparent temperature as shown by the conductivity meter agrees with that read on the water bath.

Density Measurements

An Anton Paar DMA 5000 density meter was used to measure the density of CMC salts as a function of concentration. Results are reported in the Supporting Information.

Residual Water Content Estimate

After dialysis and freeze-drying, the CMCs were exposed to air for approximately 24 h, after which approximately 15–30 mg were loaded into a Simultaneous Thermal Analyzer (STA) 6000 (PerkinElmer), heated to 120 °C, and then held for at least 20 min. The difference of the final mass relative to the initial mass was recorded for each polymer and used to estimate the water content.

■ RESULTS AND DISCUSSION

The overlap concentration (c^*) of the magnesium salt was estimated to be around 1.5 mM from viscosity measurements, using the $\eta_{sp}(c^*) \simeq 1$ criterion.[54] All the data presented below correspond to the non-dilute regime ($c > c^*$). The solubility and conductivity data as well as the scattering curves and the main parameters (correlation length and fraction of monomers with a dissociated counterion) are listed in the Supporting Information. The results presented were measured at 25 °C unless otherwise indicated. The solubility results were measured at room temperature (≃22–23 °C).

Solubility

Figure 4 plots the solubility maps of monovalent and divalent salts of CMC in the Hansen representation: δ_P represents the contribution of dipole interactions to the cohesive energy of a liquid and δ_H that of hydrogen bonding. The contribution of dispersion forces is not considered, following our earlier finding that the Hansen dispersion parameter (δ_D) does not correlate with polyelectrolyte solubility.[11] For all salts, it is observed that the polar, protic solvents such as water dissolve the polymer but apolar, aprotic solvents do not, in agreement with earlier results for various monovalent salts of CMC.[11]

The black lines in Figure 4 designate the boundaries between the soluble and insoluble regions in Hansen space. For all systems studied, the boundaries are relatively sharp, demonstrating that δ_P and δ_H are useful parameters to predict the solubility of the various salts in single solvents and mixed solvent media.

Increasing the valence of the counterion leads to a decrease in the soluble region in the Hansen plots. This is expected because as the fraction of dissociated counterions decreases, the entropic gain for dissolution becomes weaker. Increasing the counterion hydrophobicity at fixed valence (i.e., going from Cs^+ to TMA^+ or from Ca^{2+} to Hex^{2+}) increases solubility in less protic solvents.

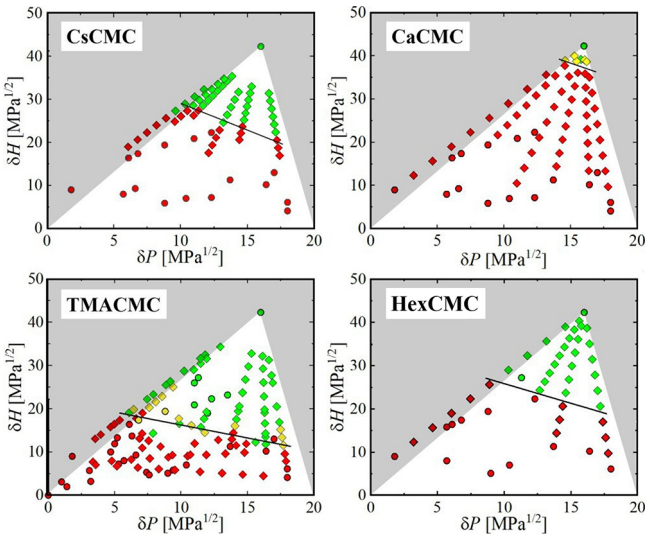

Figure 4. Hansen solubility phase maps of mono- (Cs, TMA) and divalent (Ca, Hex = hexamethonium) salts of CMC. The x-axis is the Hansen polarity parameter and the y-axis is Hansen's hydrogen bonding parameter. Circles are for pure solvents and diamonds are for mixed solvents. None of the solvents and solvent mixtures contain any added salt. Green symbols indicate soluble systems, red insoluble and yellow symbols are partially soluble, as described in the methods section. Black lines separate the soluble and insoluble regions, the method for establishing the solubility boundary is described in ref 11. Data for CsCMC and TMACMC are from ref 11. The solubility plot for SuxCMC is included in the Supporting Information.

SAXS and SANS

Influence of Metal Ion Type. The SAXS patterns for 2 wt % NaCMC and divalent metal salt solutions of CMC in DI water are shown in Figure 5. As reported in an earlier study,[4] solutions of NaCMC display a correlation peak while those of MgCMC display a broad correlation shoulder, signalling weaker local order. This is consistent with the larger fraction of condensed counterions for the divalent metal salt measured by osmotic pressure, ion-selective potentiometry and conductivity.[2,4,32]

The high/mid-q correlation shoulder in Figure 5 is seen to be approximately independent of counterion type. The exception is NiCMC, but this is probably because the contribution of the low-q upturn is still significant in the mid–q region. This suggests that the nature of the metal counterion does not influence the local conformation of CMC, see the calculation of the stretching parameter below. In an earlier study,[7] we found the chain dimensions obtained from the overlap concentration for different divalent metal salts of CMC to be independent of counterion type, which is in line with the insensitivity of the correlation length to divalent ion type observed in Figure 5.

By contrast, the excess scattering at low-q depends strongly on the identity of the counterion. The nature of the counterions influences the solubility of CMC in water. For example, the copper salt of CMC is insoluble and the barium salt is only soluble for high degrees of substitution.[7] Commercial CMC grades such as the one used in this study contain chains with a distribution of degrees of substitution.[55,56] Chains with lower

Downloaded from pubs.acs.org/mamobx/article-pdf/59/21/12025/6970982/ma-2026-01930q.pdf by OKAYAMA UNIV user on 27 November 2026

https://doi.org/10.1021/acs.macromol.6c01930
Macromolecules 2026, 59, 12025−12034

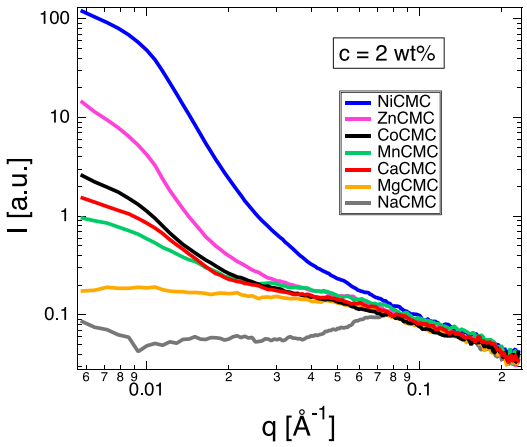

Figure 5. SAXS profiles of 2 wt % solutions of NaCMC and divalent metal salts of CMC. The counterion is indicated in the legend. Data for sodium and magnesium salts are from ref. 4. Other data are measured on the in-house instrument. Data for 1 wt % solutions are included in the Supporting Information.

substitution display lower solubility than highly substituted ones.[57] We therefore attribute the stronger low-q upturns observed for the nickel and zinc salts to large aggregates formed by weakly substituted chains, which are not fully soluble in water.

Comparison of Metal and Organic Divalent Counterions. Figure 6 compares the scattering profiles of NaCMC with those of three divalent salts, MgCMC, HexCMC, and SuxCMC, all in DI water solution without added salts. The comparison between NaCMC and MgCMC has been discussed in detail previously.[4] The transition from peak-like to shoulder-like behavior upon replacing Na^+ with Mg^{2+} is attributed to the lower effective charge density of the MgCMC salt. Conductivity and osmotic pressure data show that for MgCMC, the effective charge of the chain is approximately half that in NaCMC.[4] Although the concentration of free Mg^{2+} ions is only a quarter that of free Na^+ ions, their higher valence leads to a similar screening length ($\kappa^{-1} \simeq 1/\sqrt{4\pi l_B \Sigma_i c_i Z_i^2}$, where κ^{-1} is the Debye screening length, l_B the Bjerrum length and c_i and Z_i are the number concentration and valence of the ith ion). These effects lead to weaker inter-chain repulsion for the MgCMC salt and less local ordering on length scales of the order of the correlation length, which explains the transition between peak and shoulder behaviour.

For anisotropic counterions Sux^{2+} and Hex^{2+}, a correlation peak is observed for all concentrations studied, indicating stronger electrostatic correlations compared to the magnesium salt. As will be discussed below, this can be explained by the larger fraction of dissociated counterions compared to the magnesium or calcium salts.

Correlation Length and the Stretching Parameter. The scaling theory[58,59] predicts the correlation length of a polyelectrolyte solution to be:

$$\xi = \left(\frac{B}{bc}\right)^{1/2} \tag{1}$$

where b is the length of a monomer and c the number concentration of such monomers. B is the stretching parameter, which quantifies the degree of local folding of the polyelectrolyte. $B = 1$ corresponds to a fully stretched conformation inside the correlation blob. On distances larger than the correlation blob, electrostatics and excluded volume forces are predicted to be screened and chains should adopt random-walk statistics. Experimentally, the correlation length can be calculated from the scattering intensity as:[58,59]

$$\xi = \frac{2\pi}{q^*} \tag{2}$$

where q^* is the wave vector at the local maximum for samples that display a peak or the position of the scattering shoulder for samples which do not display a clear maximum. The position of the peak or shoulder is estimated by fitting two lines in $\log_{10}(I)$–$\log_{10}(q)$ to the high and mid-q regions of the scattering profiles and taking the intersection q between these as q^*. The values of ξ obtained from eq 2 are listed in Table S4. The final error for the correlation length was calculated by Gaussian propagation from the regression fitting error for the fit to the spectra. In practice, B was estimated by fitting a straight line with fixed zero intercept to ξ^2 vs $1/bc$.

For NaCMC, the stretching parameter is close to unity, as observed previously for many semiflexible ionic polysaccharides.[4,60] The value $B \simeq 2.3$ obtained for MgCMC indicates a modest degree of local coiling, similar to that observed in flexible polyelectrolytes with monovalent counterions, such as NaPSS[9,61] or sodium salts of maleic acid copolymers.[62] For the two ditopic organic counterions, the stretching parameter takes intermediate values of $\simeq$ 1.5–1.9, indicating a small degree of local folding. Since B is expected to correlate inversely with the effective charge of the chain, the relation $B_{Na} < B_{Sux} \lesssim B_{Hex} < B_{Mg}$ suggests that the fraction of free counterions follows the opposite order.

Small Angle Neutron Scattering. Figure 8 shows the small-angle neutron scattering intensity of HexCMC and SuxCMC solutions at 35 and 120 mM in D_2O without added salt. Since the hydrogen-rich counterions scatter more strongly than the backbone, the SANS profiles are dominated by the counterion structure factor. In contrast to the SAXS patterns, which show a clear peak, the SANS profiles display only a broad correlation shoulder, similar to that observed for concentrated TBACMC solutions in Figure 2. We interpret this as evidence that counterion and backbone concentration fluctuations are partially decoupled. Unlike CMC with monovalent tetraalkylammonium counterions, for which this decoupling was observed only at high concentrations, HexCMC and SuxCMC show no clear peak even at c = 35 mM. The available experimental evidence suggests that decoupling is favoured by counterion hydrophobicity and higher polymer concentration.[37,63] We recently reported that, for TBACMC, this decoupling is suppressed as the dielectric constant of the solvent is decreased.[31] This is intuitive because lowering the solution permittivity promotes counterion condensation. However, in HexCMC and SuxCMC, decoupling in the scattering signal is apparent even though the fraction of condensed counterions remains relatively high, ≃70% for HexCMC.

The low-q upturn is stronger in the SANS measurements than in the SAXS measurements, as observed previously for

Downloaded from pubs.acs.org/macromolecules/article-pdf/59/21/12025/6970982/ma-2026-01930q.pdf by OKAYAMA UNIV user on 27 November 2026

https://doi.org/10.1021/acs.macromol.6c01930
Macromolecules 2026, 59, 12025−12034

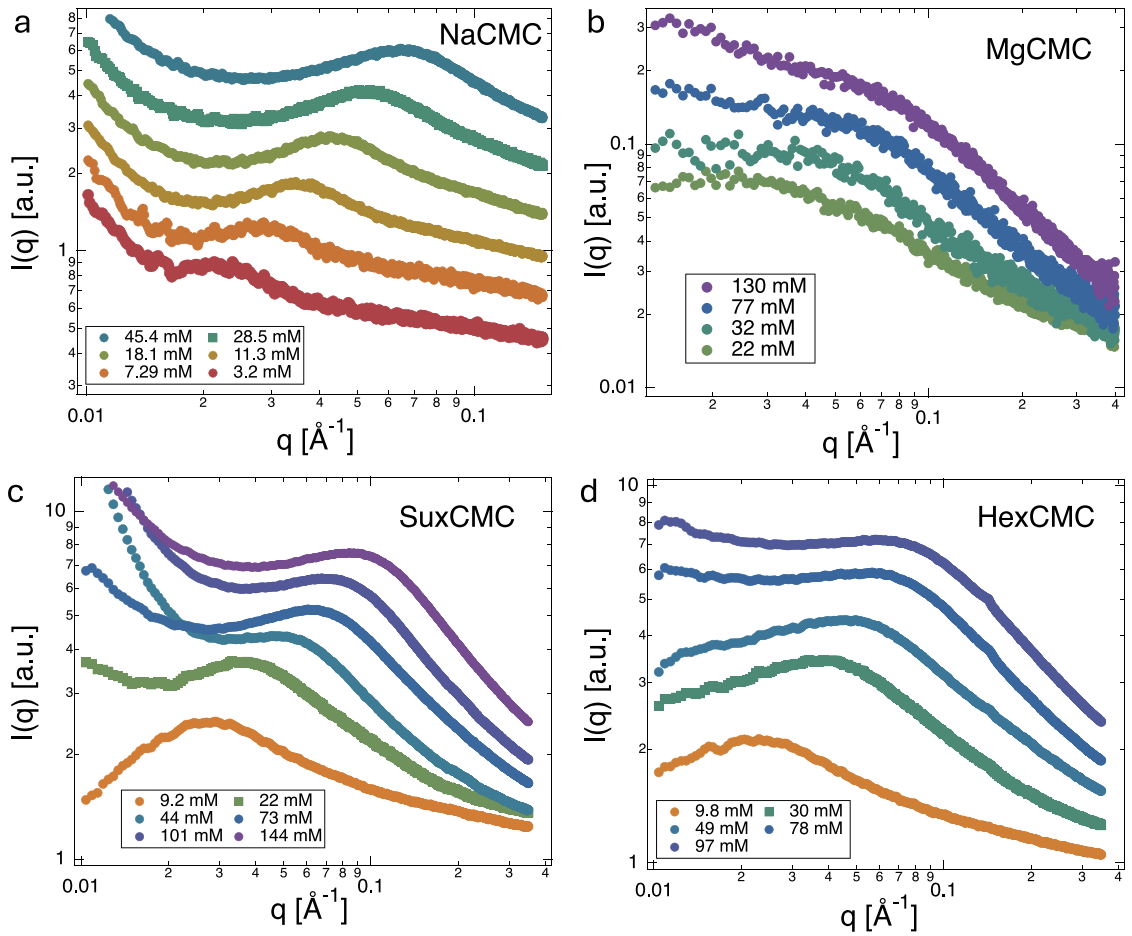

Figure 6. SAXS profiles for various salts of CMC in arbitrary units, the concentrations are indicated in the legends (a) NaCMC, (b) MgCMC, (c) SuxCMC, (d) HexCMC. The colours are chosen to correspond approximately to concentration across the different panels, such that similar colours represent the closest available concentrations for each salt. Data for the sodium salt are from ref. 50 and data for MgCMC are from ref. 4. The divalent anisotropic counterion salts display a peak while the spherical Mg salt does not. This is consistent with the lower degree of counterion condensation observed for the organic counterions, see the text.

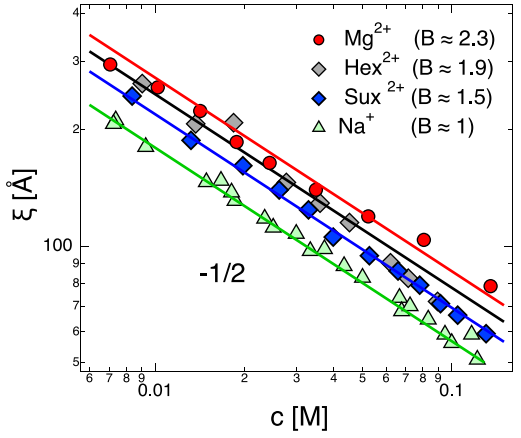

Figure 7. Correlation length as a function of polymer concentration for the salts in Figure 6. The correlation length is calculated from eq 2, where q^* is the position of the peak or of the shoulder, see ref 4 for details. The lines are fits to eq 1 with b = 5.15 Å and the best-fit B values indicated on the legend. Data for MgCMC are from ref 4 and for NaCMC are from ref 50.

MgCMC solutions.[4] The origin of this discrepancy is not presently understood, but presumably arises due to differences in contrast between SANS and SAXS.

Electrical Conductivity and Counterion Condensation

Estimating the Fraction of Free Counterions. The conductivities of the various salts of CMC are listed in Table S3. Using the model of Colby et al.,[64] the equivalent conductivity of a polyelectrolyte solution can be related to the fraction of monomers with a dissociated counterion as:

$$\Lambda = \left(\lambda_c + \frac{cf\xi^2 e^2 \ln(\xi/D)}{3\pi\eta_s}\right) f \qquad (3)$$

where λ_c is the equivalent limiting ionic conductivity of the counterion, e the electrostatic unit of charge, η_s the solvent viscosity, and D the cross-sectional diameter of the chain, taken here to be 7 Å .[65] The λ_c values of Ca^{2+}, Hex^{2+} and Sux^{2+} and the means by which they were obtained are outlined in the SI.

https://doi.org/10.1021/acs.macromol.6c01930
Macromolecules 2026, 59, 12025−12034

Downloaded from pubs.acs.org/mamobx/article-pdf/59/21/12025/6970982/ma-2026-01930g.pdf by OKAYAMA UNIV user on 27 November 2026

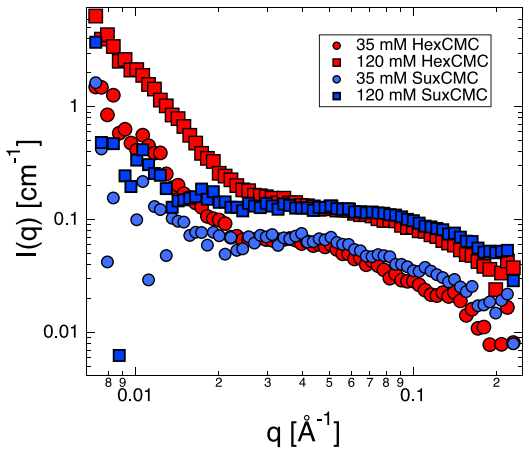

Figure 8. SANS patterns for solutions of HexCMC and SuxCMC at two different concentrations in D_2O without added salt. In contrast to the SAXS profiles, which display a clear peak, the SANS measurements display a correlation shoulder.

Eq 3 was used to estimate the fraction of free counterions of CMC salts in previous studies[4,50,66] and compared to other methods.[4] The conductivity estimates for f were ≃30% lower than the more direct measures by potentiometry or osmometry. This is in qualitative agreement with the finding of Katchalsky et al.,[67] who report that charge transport methods yield lower values for f than thermodynamic methods do. One possible reason is that eq 3 assumes that the diffusion of a free counterion is the same as that of that ion in a simple electrolyte solution in the infinite dilution limit. Experiments show that counterion diffusion is slowed down by the polyion.[68−72]

Influence of Counterion Type on the Fraction of Free Counterions. The values of f for the various CMC salts were calculated using eq 3 and the ξ data in Figure 7, and are plotted as a function of polymer concentration in Figure 9. For CaCMC we assume that the correlation length at a given molar concentration is the same as that of MgCMC. The magnesium and calcium salts display concentration-independent f values, whereas the fraction of monomers with a dissociated counterion increases with concentration for the other salts. At concentrations $c \gtrsim 0.01$ M, the order $f_{Na} > f_{Sux} \approx f_{Hex} > f_{Mg} \simeq f_{Ca}$ is consistent with the relative peak sharpness and stretching parameters obtained from SAXS.

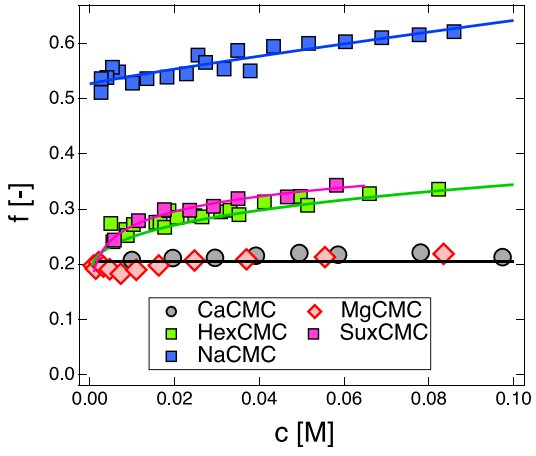

Figure 9. Fraction of monomers with a dissociated counterion as a function of polymer concentration for five salts of CMC in DI water solutions. Lines are guides to the eye. The f-values are calculated from eq 3 using the correlation length values in Figure 7.

The comparison between the organic and metal counterions does not conclusively prove that charge separation leads to enhanced dissociation because the counterions also differ in size, hydrophobicity, hydration, molecular shape, and flexibility. Several observations nevertheless suggest that the differences are unlikely to arise primarily from any one of these properties. The contour lengths of hexamethonium and suxamethonium are smaller than the Kuhn lengths of polyethylene,[73,74] a chemically analogous neutral polymer for hexamethonium, or poly(ethylene succinate),[75] which is chemically analogous to the suxamethonium backbone. In addition, the Coulomb repulsion between the charges is of the order of k_BT and should favour conformations that are slightly more extended than those of the corresponding neutral chains. We therefore conclude that counterion flexibility is unlikely to be the dominant factor.

Figure 10 shows the fraction of dissociated counterions for monovalent CMC salts as a function of counterion volume (v_{CI}). No systematic dependence on ion size is observed. Within the tetraalkylammonium series, increasing the alkyl-group size, and therefore the hydrophobicity of the counterion, also produces no systematic change in f. These results do not establish that size and hydrophobicity are unimportant for divalent counterions, rather they indicate that neither factor alone is likely to explain the enhanced dissociation of the organic divalent ions.

Hydration also appears unlikely to be the dominant origin of the observed differences. Ca^{2+} and Mg^{2+} have substantially different hydration characteristics,[24,25] but produce very similar values of f. Comparable insensitivity to counterion identity is observed among the alkali-metal salts of CMC in earlier measurements of conductivity, scattering, and chain dimensions.[4,7,30,31]

We thus conclude that the ditopic charge distribution is likely responsible for the enhanced dissociation observed for HexCMC and SuxCMC.

According to the Monte Carlo simulations of Cha et al.,[49] the condensation of rod-like, ditopic counterions can be described in terms of a distance-dependent effective valency. At distances from the polyion much larger than the separation between the two charged sites, a ditopic counterion behaves approximately

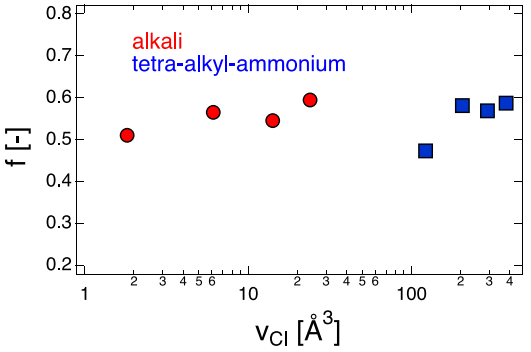

Figure 10. Fraction of monomers with a dissociated counterion as a function of counterion volume. Red symbols correspond to alkali metals and blue symbols to tetra-alkyl-ammonium ions with alkyl = Me, Et, Pr and Bu. Volumes are calculated as described in ref. 11. f is obtained by averaging values measured over a concentration range of 0.01–0.15 M for all salts. Alkali metal salt data are from ref. 4.

Downloaded from pubs.acs.org/macromol/article-pdf/59/21/12025/6970982/ma-2026-01930q.pdf by OKAYAMA UNIV user on 27 November 2026

https://doi.org/10.1021/acs.macromol.6c01930
Macromolecules 2026, 59, 12025−12034

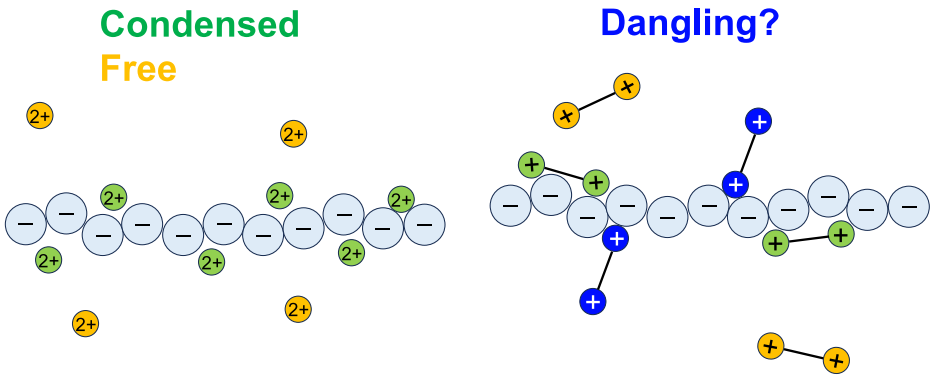

Figure 11. Schematic representation of the various states of free and condensed divalent counterions. On the left, the two states of the Oosawa-Manning theory are considered. For anisotropic counterions, a different mode of condensation is suggested.

as a single divalent point ion. At shorter distances than the separation between charges, the ions behave as two monovalent charges. This behaviour provides a possible explanation for the concentration dependence shown in Figure 9. At low concentrations, where the characteristic counterion-polyion separation is larger, the ditopic ions dissociate to a similar extent as Mg^{2+} and Ca^{2+}. At higher concentrations, the average counterion-polyion distance is smaller, and the behaviour of the ditopic ions increasingly differs from that of the monotopic divalent ions.

Dangling Condensation. An open question that cannot be fully resolved from the present data is whether separating the 2+ charge into two 1^+ centers allows the counterions to condense onto the chain without fully neutralising the charge on the backbone. An example of this hypothetical 'dangling condensation' state is illustrated schematically in Figure 11. We expect dangling counterions not to contribute significantly to the electrical conductivity of the solution because of their low mobility. Therefore, the f values calculated from eq 3 should correspond only to the free counterions. Our SAXS data indirectly support the existence of a dangling counterion state: for concentrations of ≃0.01 M, the effective charge measured from conductivity is not very different for HexCMC and Mg/CaCMC, but the former shows a correlation peak while the alkaline earth metal salts do not. This suggests a higher effective charge for the HexCMC solutions while having a similar concentration of mobile counterions. The existence of such a dangling state may be more decisively tested by dielectric spectroscopy, since the relaxation time of these local dipoles should be much shorter than that of the intermediate-frequency counterion-polarisation relaxation.

■ CONCLUSIONS

We have compared aqueous CMC solutions containing conventional divalent metal ions with those containing the organic ditopic counterions hexamethonium and suxamethonium. At low polymer concentrations, conductivity measurements indicate similar fractions of dissociated metal and ditopic counterions. At higher concentrations, the ditopic ions exhibit substantially greater counterion dissociation.

These differences are reflected in the solution structure. CMC with ditopic counterions displays correlation peaks and smaller SAXS-derived stretching parameters, consistent with a larger effective polymer charge and reduced local chain folding. By contrast, the corresponding divalent metal salts show broad correlation shoulders, indicating weaker electrostatic correlations.

The enhanced dissociation cannot be assigned uniquely to charge topology because the counterions differ not only in charge topology but also in size, hydrophobicity, and hydration. However, experimental data on other systems suggest that these last three have only a minor influence on the fraction of condensed counterions.

Partial 'dangling' condensation of the ditopic ions could explain why the SAXS profiles indicate a larger effective polymer charge even under conditions where conductivity gives similar concentrations of free counterions, but this mechanism remains conjectural. The results nevertheless demonstrate that the spatial distribution of charge within multivalent counterions can be used to tune polyelectrolyte structure and charge transport.

■ ASSOCIATED CONTENT

Supporting Information

The Supporting Information is available free of charge at https://pubs.acs.org/doi/10.1021/acs.macromol.6c01930.

Hansen solubility data, including the SuxCMC solubility map; complete SAXS and SANS scattering curves; density data for the CMC salts; conductivity, specific conductance, fraction of monomers with a dissociated charge, and correlation length data for the CMC salts (PDF)

(ZIP)

■ AUTHOR INFORMATION

Corresponding Author

Carlos G. Lopez – *Department of Materials Science and Engineering, Penn State University, University Park, Pennsylvania 16802, USA;* orcid.org/0000-0001-6160-632X; E-mail: cvg5719@psu.edu

Authors

Can Hou – *Institute of Physical Chemistry, RWTH Aachen University, Landoltweg 2, Aachen 52056, Germany*

Max Hohenschutz – *Institute of Physical Chemistry, RWTH Aachen University, Landoltweg 2, Aachen 52056, Germany;* orcid.org/0000-0002-9732-8752

https://doi.org/10.1021/acs.macromol.6c01930
Macromolecules 2026, 59, 12025−12034

Downloaded from pubs.acs.org/mamobx/article-pdf/59/21/12025/6970982/ma-2026-01930g.pdf by OKAYAMA UNIV user on 27 November 2026

Takaichi Watanabe – *Department of Applied Chemistry, Graduate School of Environmental, Life, Natural Science and Technology, Okayama University, 3-1-1, Tsushima-naka, Kita-ku, Okayama 700-8530, Japan;* orcid.org/0000-0002-5855-2583

Walter Richtering – *Institute of Physical Chemistry, RWTH Aachen University, Landoltweg 2, Aachen 52056, Germany; DWI-Leibniz Institute for Interactive Materials, Forckenbeckstr. 50, Aachen D-52056, Germany;* orcid.org/0000-0003-4592-8171

Complete contact information is available at: https://pubs.acs.org/doi/10.1021/acs.macromol.6c01930

Notes

The authors declare no competing financial interest.

■ ACKNOWLEDGMENTS

The authors are grateful to the SPring-8 synchrotron for beamtime (proposal number: 2025B1679) and Dr. Noboru Ohta (BL40B2) for his support with the SAXS experiments and data reduction. The authors thank the ISIS neutron source for beamtime (proposal number: 2690076, DOI: 10.5286/ISIS.E.RB2690076-1) and Dr. Leide Cavalcanti for conducting the SANS experiments. The authors also thank Prof. Atsushi Matsumoto and his students Marina Ikeda, Ayaka Ashie, and Tokia Maeda, as well as Alan Francisco Mejía and Lingzi Meng for providing assistance with the scattering experiments. The authors also acknowledge the DFG (RI 560/26-1) and JSPS KAKENHI (grant: JP24K01236).

■ REFERENCES

(1) Lopez, C. G.; Matsumoto, A.; Shen, A. Q. Dilute polyelectrolyte solutions: recent progress and open questions. *Soft Matter* **2024**, *20*, 2635–2687.

(2) Rinaudo, M.; Milas, M. Interaction of monovalent and divalent counterions with some carboxylic polysaccharides. *J. Polym. Sci., Polym. Chem. Ed.* **1974**, *12*, 2073–2081.

(3) Magdelenat, H.; Turq, P.; Tivant, P.; Chemla, M.; Menez, R.; Drifford, M. The effect of counter-ion substitution on the transport properties of polyelectrolyte solutions. *Biopolymers* **1979**, *18*, 187–201.

(4) GharehTapeh, E. A.; Watanabe, T.; Horkay, F.; Hou, C.; Lopez, C. G.; Hohenschutz, M. Counterion condensation, ion pairing and scattering properties of carboxymethyl cellulose with mono- and divalent ions. *Cellulose,* **2026**, *33*, 3833–3852.

(5) Zhang, Y.; Douglas, J. F.; Ermi, B. D.; Amis, E. J. Influence of counterion valency on the scattering properties of highly charged polyelectrolyte solutions. *J. Chem. Phys.* **2001**, *114*, 3299–3313.

(6) Dubois, E.; Boué, F. Conformation of poly(styrenesulfonate) polyions in the presence of multivalent ions: small-angle neutron scattering experiments. *Macromolecules* **2001**, *34*, 3684–3697.

(7) Lopez, C. G.; Richtering, W. Influence of divalent counterions on the solution rheology and supramolecular aggregation of carboxymethyl cellulose. *Cellulose* **2019**, *26*, 1517–1534.

(8) Jacobs, M.; Lopez, C. G.; Dobrynin, A. V. Quantifying the Effect of Multivalent Ions in Polyelectrolyte Solutions. *Macromolecules* **2021**, *54*, 9577–9586.

(9) Lopez, C. G.; Horkay, F.; Schweins, R.; Richtering, W. Solution properties of polyelectrolytes with divalent counterions. *Macromolecules* **2021**, *54*, 10583–10593.

(10) Ono, T.; Ohta, M.; Sada, K. Ionic Polymers Act as Polyelectrolytes in Nonpolar Media. *ACS Macro Lett.* **2012**, *1*, 1270–1273.

(11) Hou, C.; Richtering, W.; Watanabe, T.; Leonhard, K.; Papusha, M.; Lopez, C. G. Solutions of carboxymethylcellulose with organic counterions (i): The influence of counterion properties on the polymer structure and solubility. *Macromolecules* **2025**, *58*, 7489–7499.

(12) Szymczak, J.; Holyk, P.; Ander, P. Electrical conductivity of aqueous solutions of monovalent salts of polystyrenesulfonate. *J. Phys. Chem.* **1975**, *79*, 269–272.

(13) Kondou, S.; Sakashita, Y.; Morinaga, A.; Katayama, Y.; Dokko, K.; Watanabe, M.; Ueno, K. Concentrated nonaqueous polyelectrolyte solutions: high Na-ion transference number and surface-tethered polyanion layer for sodium-metal batteries. *ACS Appl. Mater. Interfaces* **2023**, *15*, 11741–11755.

(14) Okubo, T. Surface tension of synthetic polyelectrolyte solutions at the air-water interface. *J. Colloid Interface Sci.* **1988**, *125*, 386–398.

(15) Oosawa, F. *Polyelectrolytes*; Marcel Dekker, Inc., New York, NY, **1971**.

(16) Zana, R.; Tondre, C.; Rinaudo, M.; Milas, M. Étude ultrasonore de la fixation sur site des ions alcalins sur des carboxymethylcelluloses de densité de charge variable. *J. Chim. Phys.* **1971**, *68*, 1258–1266.

(17) Tondre, C.; Zana, R. Apparent molal volumes of polyelectrolytes in aqueous solutions. *J. Phys. Chem.* **1972**, *76*, 3451–3459.

(18) Tondre, C.; Zana, R. *Polyelectrolytes: Papers Initiated by a NATO Advanced Study Institute on Charged and Reactive Polymers held in France, June 1972*; Springer, *1974*; pp 323–338.

(19) Zana, R.; Tondre, C. Ultrasonic studies of polyion polyelectrolytes solutions. In *Chemical and Biological Applications of Relaxation Spectrometry: Proceedings of the NATO Advanced Study Institute Held at the University of Salford, Salford, England, 29 August–12 September, 1974*; Springer, **1975**; Vol. *18*, pp. 333–341.

(20) Komiyama, J.; Ando, M.; Takeda, Y.; Ijima, T. Dilatometric study of monovalent counter-ion association with carboxylates. *Eur. Polym. J.* **1976**, *12*, 201–207.

(21) Satoh, M.; Yoda, E.; Komiyama, J. Effects of hydrophobic hydration on counterion binding of polycations. *Macromolecules* **1991**, *24*, 1123–1127.

(22) Satoh, M.; Kawashima, T.; Komiyama, J. Competitive counterion binding and dehydration of polyelectrolytes in aqueous solutions. *Polymer* **1991**, *32*, 892–896.

(23) Koda, S.; Sugi, Y.; Sakurai, T.; Matsuoka, T.; Nomura, H. Study on segmental motion and ion binding in polyelectrolyte solutions by ultrasonic spectroscopy. *J. Solution Chem.* **2004**, *33*, 747–760.

(24) Marcus, Y.; Hefter, G. Ion pairing. *Chem. Rev.* **2006**, *106*, 4585–4621.

(25) Marcus, Y. Electrostriction in electrolyte solutions. *Chem. Rev.* **2011**, *111*, 2761–2783.

(26) Strauss, U. P.; Ross, P. D. Counterion Binding by Polyelectrolytes. IV. Membrane Equilibrium Studies of the Binding of Univalent Cations by Long-chain Polyphosphates. *J. Am. Chem. Soc.* **1959**, *81*, 5299–5302.

(27) Strauss, U. P.; Leung, Y. P. Volume changes as a criterion for site binding of counterions by polyelectrolytes. *J. Am. Chem. Soc.* **1965**, *87*, 1476–1480.

(28) Colby, R. H.; Boris, D. C.; Krause, W. E.; Tan, J. S. Polyelectrolyte conductivity. *J. Polym. Sci. B: Polym. Phys.* **1997**, *35*, 2951–2960.

(29) Marcus, Y. Tetraalkylammonium ions in aqueous and non-aqueous solutions. *J. Solution Chem.* **2008**, *37*, 1071–1098.

(30) Rinaudo, M.; Mazet, J.; Milas, M. Propriétés thermodynamiques des polyanions à densité de charge variable. *C. R. Acad. Sci.* **1973**, 1401–1404.

(31) Gulati, A.; Meng, L.; Hou, C.; Watanabe, T.; Lopez, C. G. Solution structure and counterion condensation of carboxymethyl cellulose in organic solvents. *ACS Appl. Polym. Mater.* **2026**, *8* (11): 8183–8197.

(32) Rinaudo, M. *Polyelektrolyteigenschaften von Carboxymethylcellulose in wäßriger Lösung-Einfluß der Ladungsdichte*; Faserforsch. Textiltech, **1973**, *24*(1), pp. 21–28.

(33) Rinaudo, M.; Milas, M. Propriétés électrochimiques des polyélectrolytes à densité de charge élevée. *J. Chim. Phys.* **1969**, *66*, 1489–1496.

(34) Yomota, C.; Okada, S.; Mochida, K.; Nakagaki, M. The molal osmotic coefficients and counterion activity coefficients of arabate with various counterions. *Chem. Pharm. Bull.* **1984**, *32*, 3793–3802.

Downloaded from pubs.acs.org/mamobx/article-pdf/59/21/12025/6970982/ma-2026-01930q.pdf by OKAYAMA UNIV user on 27 November 2026

(35) Satake, I.; Fukuda, M.; Ohta, T.; Nakamura, K.; Fujita, N.; Yamauchi, A.; Kimizuka, H. Interactions of counterions with dextran sulfate in aqueous solutions. *J. Polym. Sci. Polym. Phys. Ed.* **1972**, *10*, 2343–2354.
(36) Yonese, T.; Tsuge, H.; Kishimoto, H.Practical osmotic coefficients of chondroitin sulfate A and C salts with various counterions. *J. Chem. Soc. Jpn.* **1978**, *1978*, 108–112
(37) Gulati, A.; Douglas, J. F.; Matsarskaia, O.; Lopez, C. G. Influence of counterion type on the scattering of a semiflexible polyelectrolyte. *Soft Matter* **2024**, *20*, 8610–8620.
(38) Chremos, A.; Douglas, J. F. Polyelectrolyte association and solvation. *J. Chem. Phys.* **2018**, *149*, 163305.
(39) Chremos, A.; Douglas, J. F. The influence of polymer and ion solvation on the conformational properties of flexible polyelectrolytes. *Gels* **2018**, *4*, 20.
(40) Chremos, A.; Horkay, F. Disappearance of the polyelectrolyte peak in salt-free solutions. *Phys. Rev. E* **2020**, *102*, 012611.
(41) Ghosh, S.; Kundagrami, A. Effect of counterion size on polyelectrolyte conformations and thermodynamics. *J. Chem. Phys.* **2024**, *160*, 084909.
(42) Tagliabue, A.; Mella, M. The Role of Counterion Size in Defining Star-Shaped Polyelectrolytes Thermodynamics, Conformations, and Ion Dynamics. *J. Polym. Sci.* **2025**, *63*, 3005–3022.
(43) Glisman, A.; Mantha, S.; Yu, D.; Wasserman, E. P.; Backer, S.; Wang, Z.-G. Multivalent ion-mediated polyelectrolyte association and structure. *Macromolecules* **2024**, *57*, 1941–1949.
(44) Kim, Y. W.; Yi, J.; Pincus, P. Attractions between like-charged surfaces with dumbbell-shaped counterions. *Phys. Rev. Lett.* **2008**, *101*, 208305.
(45) Urbanija, J.; Bohinc, K.; Bellen, A.; Maset, S.; Iglič, A.; Kralj-Iglič, V.; Sunil Kumar, P. Attraction between negatively charged surfaces mediated by spherical counterions with quadrupolar charge distribution. *J. Chem. Phys.* **2008**, *129*, 105101.
(46) Maset, S.; Reščič, J.; May, S.; Pavlič, J. I.; Bohinc, K. Attraction between like-charged surfaces induced by orientational ordering of divalent rigid rod-like counterions: theory and simulations. *J. Phys. A: Math. Theor.* **2009**, *42*, 105401.
(47) Grime, J. M.; Khan, M. O.; Bohinc, K. Interaction between charged surfaces mediated by rodlike counterions: the influence of discrete charge distribution in the solution and on the surfaces. *Langmuir* **2010**, *26*, 6343–6349.
(48) Cha, M.; Ro, S.; Kim, Y. W. Rodlike counterions near charged cylinders: counterion condensation and intercylinder interaction. *Phys. Rev. Lett.* **2018**, *121*, 058001.
(49) Cha, M.; Ro, S.; Kim, Y. W. Condensation of rodlike counterions on a charged cylinder. *J. Korean Phys. Soc.* **2020**, *77*, 811–818.
(50) Hou, C.; Watanabe, T.; Lopez, C. G.; Richtering, W. Structure and rheology of carboxymethylcellulose in polar solvent mixtures. *Carbohydr. Polym.* **2025**, *347*, 122287.
(51) Delsanti, M.; Dalbiez, J.; Spalla, O.; Belloni, L.; Drifford, M. Phase diagram of polyelectrolyte solutions in presence of multivalent salts. In *Macro-ion Characterization: From Dilute Solutions to Complex Fluids*; Schmitz, K. S., Ed.; ACS Symposium Series 548; American Chemical Society: Washington, DC, **1994**; pp. 381–392.
(52) Raspaud, E.; Olvera de la Cruz, M.; Sikorav, J.-L.; Livolant, F. Precipitation of DNA by polyamines: a polyelectrolyte behavior. *Biophys. J.* **1998**, *74*, 381–393.
(53) Pelta, J.; Livolant, F.; Sikorav, J.-L. DNA aggregation induced by polyamines and cobalthexamine. *J. Biol. Chem.* **1996**, *271*, 5656–5662.
(54) Colby, R. H. Structure and linear viscoelasticity of flexible polymer solutions: comparison of polyelectrolyte and neutral polymer solutions. *Rheol. Acta* **2010**, *49*, 425–442.
(55) Oudhoff, K. A.; Buijtenhuijs, F. A.; Wijnen, P. H.; Schoenmakers, P. J.; Kok, W. T. Determination of the degree of substitution and its distribution of carboxymethylcelluloses by capillary zone electrophoresis. *Carbohydr. Res.* **2004**, *339*, 1917–1924.
(56) Shakun, M.; Heinze, T.; Radke, W. Determination of the DS distribution of non-degraded sodium carboxymethyl cellulose by gradient chromatography. *Carbohydr. Polym.* **2013**, *98*, 943–950.
(57) Kamide, K.; Okajima, K.; Kowsaka, K.; Matsui, T.; Nomura, S.; Hikichi, K. Effect of the distribution of substitution of the sodium salt of carboxymethylcellulose on its absorbency toward aqueous liquid. *Polym. J.* **1985**, *17*, 909–918.
(58) Dobrynin, A. V.; Colby, R. H.; Rubinstein, M. Scaling Theory of Polyelectrolyte Solutions. *Macromolecules* **1995**, *28*, 1859–1871.
(59) Dobrynin, A. V.; Rubinstein, M. Theory of polyelectrolytes in solutions and at surfaces. *Prog. Polym. Sci.* **2005**, *30*, 1049–1118.
(60) Salamon, K.; Aumiler, D.; Pabst, G.; Vuletic, T. Probing the mesh formed by the semirigid polyelectrolytes. *Macromolecules* **2013**, *46*, 1107–1118.
(61) Han, A.; Colby, R. H. Rheology of Entangled Polyelectrolyte Solutions. *Macromolecules* **2021**, *54*, 1375–1387.
(62) Di Cola, E.; Plucktaveesak, N.; Waigh, T.; Colby, R. H.; Tan, J.; Pyckhout-Hintzen, W.; Heenan, R. Structure and dynamics in aqueous solutions of amphiphilic sodium maleate-containing alternating copolymers. *Macromolecules* **2004**, *37*, 8457–8465.
(63) Combet, J.; Isel, F.; Rawiso, M.; Boué, F. Scattering functions of flexible polyelectrolytes in the presence of mixed valence counterions: condensation and scaling. *Macromolecules* **2005**, *38*, 7456–7469.
(64) Bordi, F.; Cametti, C.; Colby, R. H. Dielectric spectroscopy and conductivity of polyelectrolyte solutions. *J. Phys.: Condens. Matter* **2004**, *16* (49), 1423–1463.
(65) Lopez, C. G.; Rogers, S. E.; Colby, R. H.; Graham, P.; Cabral, J. T. Structure of sodium carboxymethyl cellulose aqueous solutions: A SANS and rheology study. *J. Polym. Sci. B: Polym. Phys.* **2015**, *53*, 492–501.
(66) Ray, D.; De, R.; Das, B. Thermodynamic, transport and frictional properties in semidilute aqueous sodium carboxymethylcellulose solution. *J. Chem. Thermodyn.* **2016**, *101*, 227–235.
(67) Katchalsky, A.; Alexandrowicz, Z.; Kedem, O. Polyelectrolyte solutions. In *Chemical physics of ionic solutions*; Conway, B. E.; Barradas, R. G., Eds.; Wiley: New York, **1966**.
(68) Lubas, W.; Ander, P. Sodium ion diffusion coefficients in aqueous salt-free polyelectrolyte solutions. *Macromolecules* **1980**, *13*, 318–321.
(69) Ander, P.; Lubas, W. Sodium ion diffusion in aqueous salt-free heparin solutions. *Macromolecules* **1981**, *14*, 1058–1061.
(70) Ander, P.; Kardan, M. Interactions of sodium ions with polyelectrolytes of constant charge density. *Macromolecules* **1984**, *17*, 2436–2441.
(71) Henningson, C. T.; Karluk, D.; Ander, P. Comparison of sodium ion interactions with sodium salts of (carboxymethyl) cellulose and vinylic polyelectrolytes of varying charge density by diffusion. *Macromolecules* **1987**, *20*, 1286–1291.
(72) Schipper, F.; Kassapidou, K.; Leyte, J. Polyelectrolyte effects on counterion self-diffusion. *J. Phys.: Condens. Matter* **1996**, *8*, 9301–9308.
(73) Schelten, J.; Ballard, D.; Wignall, G.; Longman, G.; Schmatz, W. Small-angle neutron scattering studies of molten and crystalline polyethylene. *Polymer* **1976**, *17*, 751–757.
(74) Fetters, L.; Graessley, W.; Krishnamoorti, R.; Lohse, D. Melt chain dimensions of poly (ethylene-1-butene) copolymers via small angle neutron scattering. *Macromolecules* **1997**, *30*, 4973–4977.
(75) Sasanuma, Y.; Nonaka, Y.; Yamaguchi, Y. Conformational characteristics and configurational properties of poly(ethylene succinate) and poly(butylene succinate) and structure–property–function relationships of representative biodegradable polyesters. *Polymer* **2015**, *56*, 327–339.

Downloaded from pubs.acs.org/mamobx/article-pdf/59/21/12025/6970982/ma-2026-01930q.pdf by OKAYAMA UNIV user on 27 November 2026

https://doi.org/10.1021/acs.macromol.6c01930
Macromolecules 2026, 59, 12025−12034